International Journal of Bridge Engineering (IJBE), Special Issue 2016, pp. 1-21

EFFECTS OF SECONDARY TORSION IN CURVED PRESTRESSED CONCRETE BRIDGES BUILT BY INCREMENTAL LAUNCHING METHOD

Marcello Arici[1] and Michele Fabio Granata[1]

[1] Università di Palermo, DICAM, Italy
e-mail: marcello.arici@unipa.it, michelefabio.granata@unipa.it

ABSTRACT: Incrementally launched bridges are very competitive for the construction of continuous prestressed or composite steel decks. During construction the static scheme of these bridges varies continuously, with the advancement of the deck above piers, producing temporary stresses rather different from those occurring in service life. Several of these bridges can be horizontally curved and the deck maybe composed of thin-walled sections: I-girders or boxes. Moreover curved girders are always subjected to twisting moment, associated to bending, even for dead load. In these cases the influence of non-uniform torsion becomes sizable with respect to the Saint Venant torsion, modifying the state of tangential stresses in the cross section and introducing axial stresses due to the prevented warping. In this paper an analysis method for the evaluation of non-uniform torsion effects in curved prestressed concrete girder bridges, built by the incremental launching method, is proposed. The analysis is performed by the Hamiltonian Structural Analysis method, which leads to derive directly the solution via transfer matrices. In this paper the generalized technique of Reduced Transfer Matrices is applied to the launching stages of continuous girder bridges. The comparison between two different methodologies of construction is performed. In a first case the bridge is launched with its whole concrete box section, while in a second case only a U-shape section without the upper slab is launched, in order to reduce the deck weight and the launching equipments. Results are shown on a case-study through envelope diagrams of internal forces and stresses for the entire sequence of launching. The influence of secondary torsion is addressed and the consequent variation of the state of stress is underlined.

KEYWORDS: incremental launching, bridges, non-uniform torsion, curved beams, Hamilton duality system, HSA, Reduced Transfer Matrices

1 INTRODUCTION

Continuous girder bridges can be built through the incrementally launched method [1]. This technology is currently used both for concrete and steel

girders, advancing deck segments over piers, driven from an abutment. In order to reduce the values of bending moment in the cantilever phases of advancement (fig. 1), a metallic nose is placed in front of the advancing segments. Although the more convenient section for the construction of these bridges is the box section thanks to its mechanical performance, its geometric efficiency and its effectiveness in resisting torsion and warping, nowadays I-girders open section (Π sections) are used too for bridge decks. Furthermore, this technique is applied to the construction of straight and horizontally curved bridges [2,3]. In curved bridges the effects of torsion are always coupled to bending, hence the construction stages must be analyzed taking into account twisting moment, shear force and bending moment. Moreover the cross section of these bridges is generally a thin-walled section where the effects of primary, secondary torsion and cross section distortion are always coupled.

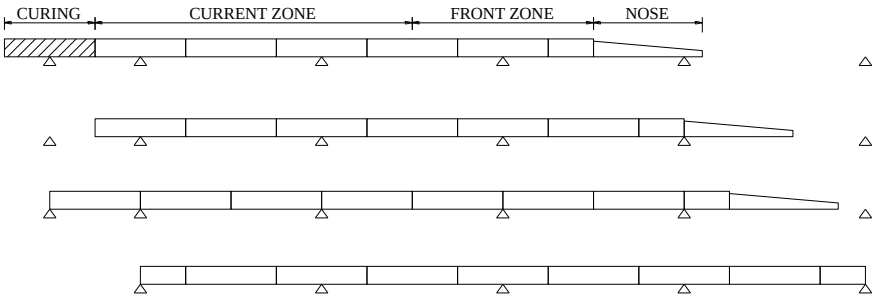

Figure 1. Launching stages

The study of thin-walled structures was initially carried out by Vlasov [4] for the case of open sections, introducing the theory of sectorial coordinates; afterwards important contributions were given by Dabrowski [5] while Bažant [6] presented a theoretical study developing different approaches for open and closed cross sections. Sedlacek [7] proposed a comprehensive theory for considering torsional warping and distortional effects in single and multi-cell box girders and decisive contributions were given in the book by Kollbrunner & Basler [8]. Kollbrunner and Hajdin [9] extended the Vlasov theory and the theory of folded plates through an analytical model which takes into account torsional and distortional warping for deformable thin-walled sections. A unified approach for analysing secondary torsion in beams with open and closed sections was proposed by Guo Zhong-heng [10] while other researchers, such as Bažant & El-Nimeiri [11] and Razaqpur & Li [12], implemented the theory of non-uniform torsion in finite element procedures in order to analyse curved girder structures with thin-walled sections. Nakai & Yoo [13] proposed a wide study on the analysis and design of curved steel bridges. Non-uniform torsion,

distortion and shear lag of concrete box sections of straight bridges were considered by Maisel [14] through a matrix method in which the governing differential equations of the problem are decoupled. Recently several studies try to take into account the shear deformation of the cross-section midline in warping torsion [15,16]. FEM models [17] and BEM models [18], based on the Secondary Torsion Moment Deformation Effect (STMDE), were developed for 3D beams taking into account warping torsion. Methods based on finite and boundary elements may be computationally heavy when they take these phenomena into account, particularly for curved bridges, and often it is difficult in engineering practice to deal with those tools, especially when they are predefined closed numerical packages. In the case of construction by incremental launching this difficulty increases very much due to the number of stages to be analysed, making these numerical methods practically not suitable of application for current engineering design purposes.

In curved bridges the contribution of non-uniform torsion is very significant, because bending and torsion are always coupled. In addition, the curved bridges, together with the torsion, may be suffering from distortion (loss of section shape) and from the phenomena related to the shear-lag.

The analysis of thin-walled sections together to the advancing stage-construction analysis makes necessary the evaluation of a large number of static schemes, one for each phase of progress, until reaching the final configuration, so that the designer is able to extract the envelope of the stress diagrams for evaluating the behavior of the bridge in all stages of advancement [1,2].

For this reason in the present study, the solution of construction stages is obtained using the Hamiltonian Structural Analysis (HSA) method, based on an energetic approach and the definition of the Hamiltonian potential function [19]. The method is fast and useful for repetitive calculations, avoiding the construction of 3D FEM models, which may be computationally too onerous.

The Hamiltonian Structural Analysis (HSA) method, for one-dimensional structures in 3D-space, starts from the principle of stationary total potential energy through the Legendre transformation, which is applied to the total potential energy density. The total potential energy density represents the Lagrange function which is transformed into a Hamiltonian function, that is a mixed energy density. The canonical Hamiltonian system, which expresses the solution system of the elastic problem, is expressed through differential equations of the 1st order and the solution of the canonical dual system is a mixed state array of displacements and stress resultants, associated to the appropriate boundary conditions. Moreover the fundamental matrix of the solving system coalesces to the transfer matrix of the structure. Hence the transfer matrix method can be applied as powerful tool to avoid complex and time consuming solving procedures.

The HSA method can be applied to thin-walled structures by introducing the appropriate kinematical degrees of freedom and the corresponding compatibility

equations [19]. Hence non-uniform torsion for rigid cross-sections as well as distortion (deformable cross section), shear lag, temperature distributions inside the sections and other problems can be solved directly, by finding the expression of the Hamiltonian function and by approaching the variational formulation. This is a convenient method which maintains a solving system with a number of equations always double the number of kinematical degrees of freedom introduced in the formulation.

The HSA method can be seen in the frame of a general method of analysis of physical systems, developed by Zhong [20], which is based on the analogy relationships between structural mechanics and optimal control. In structural mechanics the field compatibility equations, together with field equilibrium equations, form a natural duality system that can be directly obtained from the Hamilton function, termed as density of mixed energy. In fact the Hamilton form of dual equations in structural mechanics and the dual equation system in optimal control theory are analogous to each other mathematically. The elastic problem can be seen on the dynamical point of view when the coordinate is the time and on the static point of view, when the coordinate is spatial, like the continuous abscissa of the structural axis joining cross section centroids of a continuous body.

In the following HSA method is presented for the solution of horizontally curved beams with open or closed thin-walled cross section having Π shape or one-cell box section. When the angle of twist per unit length is not constant, the Saint-Venant theory of torsion is not reliable in thin-walled sections and the evaluation of non-uniform torsion is essential; in this connection additional axial stresses rise in web and flanges of cross section due to warping. Parametric analysis of continuous curved bridges through HSA is reported in [21]. Cross section deformation and shear lag have to be considered associated to torsion [19] for evaluating the variations of axial stresses with respect to the Saint-Venant theory. The presence of stiffeners and bracing inside cross sections limits distortional effects, while rigid diaphragms can increase axial stresses due to torsional and distortional warping.

In this paper a study of the construction stages of a prestressed concrete bridge, horizontally curved, with a closed box section is presented. Two different and alternative construction methodologies are examined. In the first the full box is launched over span lengths of 46 m, studying the effect of the geometric curvature and of the non-uniform torsion in the case of thin-walled box sections. Being a prestressed concrete deck with the full section very heavy and with expensive launching technology required together with an onerous temporary prestressing. Alternatively, to reduce the problems of pushing forces and the weight of the cross section, it is considered a second hypothesis of construction in which only a reduced U-shape section is advanced, concreting the upper slab after the launch is completed. In this case, an open section occurs

and its stiffness is significantly lower than the previous case of box section, being not possible to keep the span length to 46 m. Thus it was evaluated the possibility of using intermediate temporary piers, reducing the span length to the half and consequently reducing the equipment and technology necessary for launching and the temporary prestressing to be adopted in the launching phase. It should of course carefully consider the additional costs of temporary piers and the largest number of intermediate supports, which should, however, be offset by the simple implementation of the pushing force and of the provisional prestressing. In both cases torsion (and more precisely non-uniform torsion) plays a very important role because in the first case it acts on a closed section which is complete and with optimum mechanical properties (definitive section and longer spans), while in the second case acts to a thin walled open section, much more sensitive to the secondary effects of non-uniform torsion (temporary open section and shorter spans).

The solution of incrementally launched straight bridges was developed by Rosignoli [22] through the transfer matrices (TMM). Sasmal et al. [23] extended the methodology and assessed the interaction between the nose and the deck. Recently, the problem of nose optimization has also been studied by Fontan et al. [24], with advanced optimization techniques. Other works extended this analysis methodology to curved bridges, evaluating the global behavior [25] but only for primary torsion. The authors demonstrated that TMM can be considered as a special case of the more general Hamiltonian Structural Analysis (HSA) method. A parametric study of curved beams with various open and closed cross-sections is presented in [25] and a study of non-uniform torsion effects on continuous bridges built by incrementally launching, with different cross sections, is given in [26]. This method is applied here to the solution of the incremental launching stages, taking into account the effects of non-uniform torsion. The result is the formulation of a theory of a generalized beam that allows the designer to calculate the stress state in the construction phases, which are also the most complex.

2 SOLUTION OF CURVED BRIDGES WITH NON-UNIFORM TORSION BY THE HSA METHOD

In this section the HSA method is applied to girder bridges curved in the plane, taking into account secondary torsion. The general theory can be found in [19].
For a horizontally curved beam (figure 2), whose axis lies on a horizontal plane, in the generic section of curvilinear coordinate s, with the local coordinate system given by the Frenet unit vectors $\boldsymbol{i}_1$, $\boldsymbol{i}_2$, $\boldsymbol{i}_3$ (respectively along the normal, binormal and tangent axes to the curve) placed in the cross-section centroid (G), it is possible to define an array $\boldsymbol{u}(s)$ and an array $\boldsymbol{Q}(s)$ containing the displacement and internal force components:

$$\boldsymbol{u}(s)=\left(u_2,\varphi_1,\varphi_3,\zeta_3\right)^{\mathrm{T}};\ \ \boldsymbol{Q}(s)=\left(V_2,M_1,M_3,B_3\right)^{\mathrm{T}} \tag{1}$$

where u_2 is the vertical displacement, φ_1 the bending rotation, φ_3 the angle of twist around the shear centre (C), ζ_3 the warping intensity function, V_2 the shear force, M_1 the bending moment, M_3 the twisting moment defined respect to the shear centre. B_3 is the internal force related to warping, called bimoment (or warping moment).

In non-uniform torsion of thin walled curved beams the total twisting moment M_3 consists of a contribution from Saint Venant torsion M_d and of a contribution from the torsional warping moment M_ω which is the derivative of bimoment B_3:

$$M_3=M_d+M_\omega=GJ\left(\frac{d\varphi_3}{ds}-\frac{\varphi_1}{R}\right)+\frac{dB_3}{ds} \tag{2}$$

The field compatibility and equilibrium equations of the curved beam with non-uniform torsion are the following:

$$\begin{cases}\dfrac{du_2}{ds}=\chi_2\dfrac{V_2}{GA}-\varphi_1\\ \dfrac{d\varphi_1}{ds}=\dfrac{M_1}{EJ_1}-\dfrac{1}{R}\varphi_3\\ \dfrac{d\varphi_3}{ds}=-\kappa\,\zeta_3+\dfrac{1}{R}\varphi_1+\dfrac{M_3}{GJ_C}\\ \dfrac{d\zeta_3}{ds}=\dfrac{B_3}{EI_\omega}\end{cases}\qquad\begin{cases}\dfrac{dV_2}{ds}=-p_2\\ \dfrac{dM_1}{ds}=V_2-m_1-\dfrac{M_3}{R}\\ \dfrac{dM_3}{ds}=-m_3+\dfrac{M_1}{R}\\ \dfrac{dB_3}{ds}=\kappa\,M_3+\kappa\,GJ\,\zeta_3\end{cases} \tag{3a,b}$$

where E is the Young elastic modulus, G is the shear modulus, R is the constant curvature radius, m_3 is the distributed torque, χ_2 is the shear factor, A is the cross section area, J_1 is the moment of inertia, J_C is the torsional polar moment of inertia of cross section and I_ω is the torsional warping constant, both defined with respect to shear centre:

$$J_C=\int r^2 t\,ds_w\ ,\quad I_\omega=\int_A \omega^2 t\,ds_w \tag{4a,b}$$

in which ω is the sectorial area (or normalized sectorial coordinate) of thin-walled open or closed sections, r is the distance from the shear centre to the tangent to the midline of the thin-walled section profile, t is the thickness of the section wall and s_w is the curvilinear coordinate along the profile midline. For one-cell rectangular or trapezoidal box sections, normalized sectorial coordinate ω_{closed} is obtained cutting the closed cell and considering the warping function of the derived open section ω_{open}, detracting the contribution of the shear flow, according to the following relation:

$$\omega_{closed} = \omega_{open} - \frac{J}{\Omega}\int_0^{s_w} \frac{ds_w}{t} \tag{4c}$$

where J is the torsional constant for closed sections and Ω is the double of the area closed by the profile midline.

In eq. (3a) M_1/EJ_1, M_3/GJ_C and B_3/EI_ω are respectively the bending, torsional and bimoment mechanical curvatures while in eq. (3b) p_2 is the distributed vertical load. In eqs. (3) constant κ is defined by:

$$\kappa = 1 - \frac{J}{J_C}; \quad J_C = \frac{J}{1-\kappa} \tag{5}$$

For box sections, J is the Bredt torsional constant and it is not much smaller than J_C; by contrast for open sections, the Saint-Venant torsional constant J is much smaller than J_C, being $J/J_C \rightarrow 0$. The value of the shear parameter κ distinguishes the behaviour of different kinds of cross-section: $\kappa << 1$ for box sections and $\kappa < 1$ for open sections. This parameter is a discriminant of cross section behaviour in the unified theory, being $\kappa \rightarrow 0$ and $J/J_C \rightarrow 1$ for compact sections.

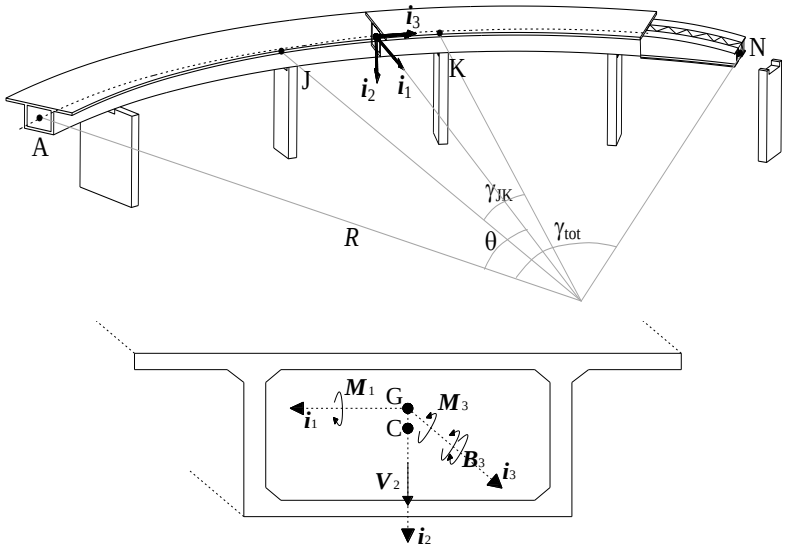

Figure 2. Curved continuous girder bridge, generic J-K span and box cross section with local axes.

In the frame of HSA [19], the equilibrium and compatibility equations (3) maybe compacted in matrix form through a canonical Hamiltonian dual system of 1st order differential equations.

$$\begin{cases} \boldsymbol{u}' = -\boldsymbol{B}\,\boldsymbol{u}(s) + \boldsymbol{E}^{-1}\boldsymbol{Q}(s) + \boldsymbol{q}_e(s) = \dfrac{\partial H}{\partial \boldsymbol{Q}} \\ \boldsymbol{Q}' = \boldsymbol{B}^T\boldsymbol{Q}(s) + \boldsymbol{R}\,\boldsymbol{u}(s) - \boldsymbol{f}_e(s) = -\dfrac{\partial H}{\partial \boldsymbol{u}} \end{cases} \tag{6}$$

where $\boldsymbol{B}$ is a geometric gradient matrix of displacements (referred to the compatibility equations), $\boldsymbol{E}^{-1}$ is the diagonal flexibility matrix containing the mechanical constants (i.e. the inverse of the stiffness matrix) for a beam having constant cross-section with an axis of symmetry along $\boldsymbol{i}_2$. $\boldsymbol{R}$ is a matrix that characterizes a fictitious elastic soil and in this case it contains the parameter linked to the Saint-Venant torsion.

In the previous equations $\boldsymbol{f}_e(s) = (p_2(s),\ m_1(s),\ m_3(s),\ 0)^{\mathrm{T}}$ is the array of distributed external loads and $\boldsymbol{q}_e(s) = (0, 0, 0, 0)^{\mathrm{T}}$ is the array of imposed strains (e.g. imposed curvature induced by a temperature gradient), being the latter a null array in this case. H is a mixed energy density function (the Hamiltonian function) linked to the total potential energy density of the beam, with several important properties. By collecting $\boldsymbol{f}_e(s)$ and $\boldsymbol{q}_e(s)$ in a mixed generalized external action array and by collecting $\boldsymbol{u}(s)$ and $\boldsymbol{Q}(s)$ in a mixed state array

$$\boldsymbol{d}_e(s) = [\boldsymbol{f}_e{}^{\mathrm{T}}(s),\ \boldsymbol{q}_e{}^{\mathrm{T}}(s)]^{\mathrm{T}} \quad ; \quad \boldsymbol{z}(s) = [\boldsymbol{u}^{\mathrm{T}}(s),\ \boldsymbol{Q}^{\mathrm{T}}(s)]^{\mathrm{T}} \tag{7}$$

the Hamiltonian function assumes the form of a sum of two terms, one quadratic and one linear:

$$H(\boldsymbol{z}) = \frac{1}{2}\boldsymbol{z}^T(s)\,\boldsymbol{A}(s)\boldsymbol{z}(s) + \boldsymbol{d}_e^T(s)\boldsymbol{z}(s) \tag{8}$$

where

$$\boldsymbol{A} = \begin{bmatrix} -\boldsymbol{R} & -\boldsymbol{B}^{\mathrm{T}} \\ -\boldsymbol{B} & \boldsymbol{E}^{-1^{\mathrm{T}}} \end{bmatrix} = \left[\begin{array}{cccc:cccc} 0 & 0 & 0 & 0 & 0 & 0 & 0 & 0 \\ 0 & 0 & 0 & 0 & -1 & 0 & \dfrac{1}{R} & 0 \\ 0 & 0 & 0 & 0 & 0 & -\dfrac{1}{R} & 0 & 0 \\ 0 & 0 & 0 & -\kappa GJ & 0 & 0 & -\kappa & 0 \\ \hdashline 0 & -1 & 0 & 0 & \dfrac{\chi_2}{GA} & 0 & 0 & 0 \\ 0 & 0 & -\dfrac{1}{R} & 0 & 0 & \dfrac{1}{EJ_1} & 0 & 0 \\ 0 & \dfrac{1}{R} & 0 & -\kappa & 0 & 0 & \dfrac{(1-\kappa)}{GJ} & 0 \\ 0 & 0 & 0 & 0 & 0 & 0 & 0 & \dfrac{1}{EI_\omega} \end{array}\right] \tag{9}$$

Eq. (6) can be expressed by the following canonical dual symplectic system of 1st order differential equations:

$$\frac{d\boldsymbol{z}(s)}{ds} = \boldsymbol{J}\frac{dH(\boldsymbol{z})}{d\boldsymbol{z}} = \boldsymbol{J}\left[\boldsymbol{A}\,\boldsymbol{z}(s) + \boldsymbol{d}_e(s)\right] \tag{10}$$

where $\boldsymbol{J}$ is the skew symmetric symplectic operator and $\boldsymbol{I}$ is the 4×4 identity matrix

$$\boldsymbol{J} = \begin{bmatrix} \boldsymbol{0} & \boldsymbol{I} \\ -\boldsymbol{I} & \boldsymbol{0} \end{bmatrix} \tag{11}$$

The solution of eq. (10) is given by the fundamental matrix $\boldsymbol{C}(s)$ of the homogeneous system and it expresses the relation between the state array in s = 0 and the one in the generic section of abscissa s, in the following form:

$$\boldsymbol{z}(s) = \boldsymbol{C}(s)\,\boldsymbol{z}(0) + \boldsymbol{N}(s) \tag{12}$$

where $\boldsymbol{C}(s)$ depends on the geometrical and mechanical characteristics of the beam and $\boldsymbol{N}(s)$ expresses the effects of external actions along the beam axis. For a horizontal plane curved beam the expression of the 8×8 fundamental matrix can be found by the exponential matrix

$$\boldsymbol{C}(s) = \boldsymbol{exp}\,(\boldsymbol{J}\,\boldsymbol{A}\,s) = \boldsymbol{I} + \boldsymbol{J}\boldsymbol{A}\,s + \left(\boldsymbol{J}\boldsymbol{A}\,s\right)^2/2! + \left(\boldsymbol{J}\boldsymbol{A}\,s\right)^3/3! + \ldots + \left(\boldsymbol{J}\boldsymbol{A}\,s\right)^n/n! + \ldots \tag{13}$$

while the effects of external actions (distributed loads and possible imposed strains on the beam) can be taken into account by the array $\boldsymbol{N}(s)$:

$$\boldsymbol{N}(s) = \int_0^s \boldsymbol{C}(s-\eta)\,\boldsymbol{J}\,\boldsymbol{d}_e(\eta)\,d\eta \tag{14}$$

Once the transfer matrix $\boldsymbol{C}(s)$ has been defined (and calculated via precise integration method [20]), it is possible to expand it by adding one more column and one more row, in order to include array $\boldsymbol{N}(s)$ and the general expression (12) can be written in a compact form:

$$\boldsymbol{S}(s) = \begin{pmatrix} \boldsymbol{z}(s) \\ 1 \end{pmatrix} = \left[\begin{array}{c:c} \boldsymbol{C}(s) & \boldsymbol{N}(s) \\ \hdashline \boldsymbol{0}^{\mathrm{T}} & 1 \end{array}\right] \begin{pmatrix} \boldsymbol{z}(0) \\ 1 \end{pmatrix} = \boldsymbol{F}(s)\,\boldsymbol{S}(0) \tag{15}$$

where $\boldsymbol{S}(s)$ is the expanded state array and $\boldsymbol{F}(s)$ is the expanded transfer matrix for the generic section s. Therefore, the relation between the state arrays of two subsequent sections J and K can be expressed by the 9×9 matrix $\boldsymbol{F}_{\mathrm{JK}}$:

$$\boldsymbol{S}_{\mathrm{K}} = \boldsymbol{F}_{\mathrm{JK}}\,\boldsymbol{S}_{\mathrm{J}} \tag{16}$$

If a circular curved beam on rigid radial supports with constant curvature radius R is considered, the curvilinear coordinate of the generic section is $s = R\theta$ and $L=R\gamma_{\mathrm{tot}}$ the total beam length from section A to section N at the end of the beam, with spans each of length $l_{\mathrm{JK}}=R\gamma_{\mathrm{JK}}$ between two subsequent supports J and K (figure 2).

In each section a point matrix $\boldsymbol{P}_{\mathrm{I}}$ can be defined to take into account concentrated discontinuities. The 9$^{\mathrm{th}}$ order matrix $\boldsymbol{P}_{\mathrm{I}}$ is composed of a 8$^{\mathrm{th}}$ order

identity matrix and of a 8th order column containing the terms of concentrated discontinuities:

$$\boldsymbol{P}_{\mathrm{I}} = \begin{bmatrix} \boldsymbol{I}_8 & \Delta\boldsymbol{z} \\ \boldsymbol{0}^T & 1 \end{bmatrix}, \quad \Delta\boldsymbol{z} = \left(\Delta u_2 \; \Delta\varphi_1 \; \Delta\varphi_3 \; \Delta\zeta_3 \; \Delta V_2 \; \Delta M_1 \; \Delta M_3 \; \Delta B_3 \right)^T \tag{17}$$

being $\boldsymbol{I}_8$ a 8×8 identity matrix. By considering discontinuities, the state array $\boldsymbol{S}_{\mathrm{N}}$ at the end section of the curved beam can be expressed as a function of the state array $\boldsymbol{S}_{\mathrm{A}}$ at the initial section, by the recursive formula:

$$\boldsymbol{S}_{\mathrm{N}} = \boldsymbol{F}_{\mathrm{A}}^{\mathrm{N}} \boldsymbol{S}_{\mathrm{A}} = \boldsymbol{P}_{\mathrm{N+1}} \boldsymbol{F}_{\mathrm{N-1}}^{\mathrm{N}} \boldsymbol{P}_{\mathrm{N}} \boldsymbol{F}_{\mathrm{N-2}}^{\mathrm{N-1}} \boldsymbol{P}_{\mathrm{N-1}} \ldots \boldsymbol{F}_{\mathrm{A}}^{\mathrm{B}} \boldsymbol{P}_{\mathrm{A}} \boldsymbol{S}_{\mathrm{A}} \tag{18}$$

The system of eq. (18), which is valid for the whole structure, can be solved by imposing the boundary conditions at the ends of the beam, by partitioning the coefficient matrix of the 8th order.

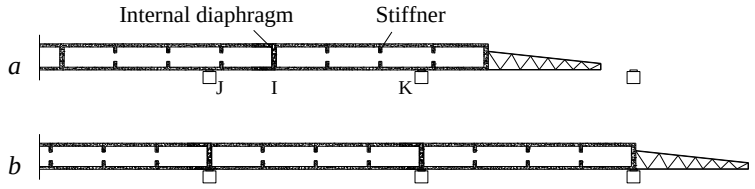

Figure 3. Bearings on piers and diaphragms locations during deck advancement

When discontinuities are unknown as it occurs over supports of a continuous beam, equation (17) contains some redundant unknowns (support reaction discontinuities ΔV_2, ΔM_3 and ΔB_3), so the system (18) can be solved by implementing the so-called reduced transfer matrix method [26]. The aim of this method is to find a reduced solving system by excluding the unknown variables and by identifying the variables which are continuous along the beam. In fact each matrix $\mathbf{P}_{\mathrm{K}}\mathbf{F}_{\mathrm{JK}}$ contains redundant unknowns. By considering the case of free warping over piers, each matrix $\mathbf{F}_{\mathrm{JK}}$ can be partitioned by separating known variables from unknowns, defining arrays $\mathbf{K}_{\mathrm{J}} = (u_2 \; \varphi_3)_{\mathrm{J}}^{\mathrm{T}}$ and $\mathbf{K}_{\mathrm{K}} = (u_2 \; \varphi_3)_{\mathrm{K}}^{\mathrm{T}}$ of known variables at support sections and arrays $\mathbf{U}_{\mathrm{J}} = (V_2 \; M_3)_{\mathrm{J}}^{\mathrm{T}}$ and $\mathbf{U}_{\mathrm{K}} = (V_2 \; M_3)_{\mathrm{K}}^{\mathrm{T}}$ of unknown variables. Continuous variables upon each support can be placed in arrays $\mathbf{z}_{\mathbf{RJ}} = (\varphi_1 \; \zeta_3 \; M_1 \; B_3)_{\mathrm{J}}^{\mathrm{T}}$ and $\mathbf{z}_{\mathbf{RK}} = (\varphi_1 \; \zeta_3 \; M_1 \; B_3)_{\mathrm{K}}^{\mathrm{T}}$.

The equilibrium and compatibility conditions to be fulfilled at the left and right sides of an internal support are the ones linking the continuous variables collected in the array $\mathbf{z}_{\mathbf{RJ}}$ of the i-th span, to those of the array $\mathbf{z}_{\mathbf{RK}}$ of the (i-1)th span (e.g. equal values of rotations and/or moments at left and right sides of supports). Under these hypotheses the solving system of a span J-K can be rearranged:

$$\begin{pmatrix} \mathbf{K}_K \\ \mathbf{U}_K \\ \mathbf{z}_{RK} \\ 1 \end{pmatrix} = \begin{bmatrix} \mathbf{F}_{11} & \mathbf{F}_{12} & \mathbf{F}_{13} & \mathbf{F}_{14} \\ \mathbf{F}_{21} & \mathbf{F}_{22} & \mathbf{F}_{23} & \mathbf{F}_{24} \\ \mathbf{F}_{31} & \mathbf{F}_{32} & \mathbf{F}_{33} & \mathbf{F}_{34} \\ \mathbf{0}^T & \mathbf{0}^T & \mathbf{0}^T & 1 \end{bmatrix} \begin{pmatrix} \mathbf{K}_J \\ \mathbf{U}_J \\ \mathbf{z}_{RJ} \\ 1 \end{pmatrix} \tag{19}$$

From the first row of equation (19), by solving it with respect to the unknown elements $\mathbf{U}_J$,

$$\mathbf{U}_J = \mathbf{F}_{12}^{-1}\left(\mathbf{K}_K - \mathbf{F}_{11}\mathbf{K}_J - \mathbf{F}_{13}\mathbf{z}_{RJ} - \mathbf{F}_{14} \right) \tag{20}$$

while, from the third row of eq. (19), one obtains

$$\mathbf{z}_{RK} = \mathbf{G}_{JK}\mathbf{z}_{RJ} + \mathbf{G}_{NJK} \tag{21}$$

in which

$$\begin{aligned} \mathbf{G}_{JK} &= \mathbf{F}_{33} - \mathbf{F}_{32}\mathbf{F}_{12}^{-1}\mathbf{F}_{13} \\ \mathbf{G}_{NJK} &= \mathbf{F}_{31}\mathbf{K}_J + \mathbf{F}_{32}\mathbf{F}_{12}^{-1}\left(\mathbf{K}_K - \mathbf{F}_{11}\mathbf{K}_J - \mathbf{F}_{14} \right) + \mathbf{F}_{34} \end{aligned} \tag{22}$$

By inserting $\mathbf{G}_{NJK}$ and $\mathbf{G}_{JK}$ into a reduced transfer matrix $\mathbf{F}_{RJK}$

$$\mathbf{F}_{RJK} = \begin{bmatrix} \mathbf{G}_{JK} & \mathbf{G}_{NJK} \\ \mathbf{0}^T & 1 \end{bmatrix} \tag{23}$$

and by considering the reduced state array $\mathbf{S}_R = (\varphi_1\ \zeta_3\ M_1\ B_3\ 1)^T$, a compact expression of equation (21) can be found, obtaining the reduced system

$$\mathbf{S}_{RK} = \mathbf{F}_{RJK}\ \mathbf{S}_{RJ} \tag{24}$$

where $\mathbf{F}_{RJK}$ is the 5×5 *reduced transfer matrix* of the J-K segment between two subsequent supports. Elements of the reduced transfer matrix $\mathbf{F}_{RJK}$ are obtained directly as a combination of those of transfer matrix $\mathbf{F}_{JK}$. In this way, if the entire continuous beam between A and N is considered, the reduced solving system is:

$$\mathbf{S}_{RN} = \mathbf{F}_{RA,N}\mathbf{S}_{RA,N} = \mathbf{F}_{R\,N\text{-}1,N}\mathbf{F}_{R\,N\text{-}2,N\text{-}1}\ldots\mathbf{F}_{R\,A,B}\mathbf{S}_{RA} \tag{25}$$

This reduced system can be solved by imposing the boundary conditions at joints A and N (e.g. known values of bending moments and bimoment). After the reduced system is solved, all values of bending moment, bimoment, rotation and warping for every support can be found. Finally, by substituting the values of $\mathbf{S}_{RJ}$ and $\mathbf{S}_{RK}$ in equation (24), the continuous beam can be finally solved by defining the complete system of equation (18) and the state arrays $\mathbf{S}_J$ and $\mathbf{S}_K$ can be found for each girder segment.

This solution is correct when warping is free along the entire deck; actually, diaphragms which prevent torsional warping can be placed at intermediate sections and this complicates the solution of the continuous beam during launching because the position of the diaphragms varies at each step of advancement (fig. 3). In the diaphragm section warping is prevented, so the

variable ζ_3 is nullified and bimoment B_3 is an unknown variable. In the general situation shown in figure 3*a*, the reduced transfer matrix between supports J and K has to take into account the presence of the intermediate section I with the diaphragm, in which the value of bimoment is unknown. To do this, it is sufficient to divide the reduced matrix of the span J-K into two sub-matrices, whose elements are reordered depending on the known, unknown and continuous variables at the extremes J, I and K. In this case in fact, the sub-arrays of eq. (19) become: $\mathbf{K}_J = (u_2\ \varphi_3)_J^T$, $\mathbf{K}_I = (\zeta_3)_I^T$, $\mathbf{K}_K = (u_2\ \varphi_3)_K^T$ for known variables, $\mathbf{U}_J = (V_2\ M_3)_J^T$, $\mathbf{U}_I = (B_3)_I^T$, $\mathbf{U}_K = (V_2\ M_3)_K^T$ for unknown variables and $\mathbf{z_{RJ}} = (\varphi_1\ \zeta_3\ M_1\ B_3)_J^T$, $\mathbf{z_{RI}} = (u_2\ \varphi_1\ \varphi_3\ V_2\ M_1\ M_3)_I^T$, $\mathbf{z_{RK}} = (\varphi_1\ \zeta_3\ M_1\ B_3)_K^T$ for continuous variables. In this way the reduced matrix of span J-K is given by the product of sub-matrices of segments I-K and J-I: $\mathbf{F}_{\mathbf{R}JK} = \mathbf{F}_{\mathbf{R}IK}\mathbf{F}_{\mathbf{R}JI}$, each sub-matrix referring to the continuous variables of the extremes J, I and K. Once the unknown variables at J and K sections are found solving eq. (25), values of bimoment at the left and right sides of the I section can be evaluated too. The reduced transfer matrix of the span J-K has to be divided in two sub-matrices till the diaphragms are placed over piers (position of figure 3*b*), when the span coincides with the mutual distance of diaphragms.

The state of stress of cross section is due to the following internal forces:

1) axial force N_x (mainly due to temporary prestressing), longitudinal shear force V_2, longitudinal bending moment M_1 (inclusive of bending due to prestressing) and total twisting moment M_3;
2) torsional warping (bimoment B_3 and secondary torsion M_ω);

Summarizing the contributions to the longitudinal axial stress, in a generic fibre of cross section, the following relation is established:

$$\sigma_x = \frac{N_x}{A} + \frac{M_1}{I_1} y + \frac{B_\omega}{I_\omega}\omega \tag{26}$$

where y the generic distance of the concrete fibre from cross section centroid.
In the same way, the value of tangential stress in the web can be evaluated through the following expression:

$$\tau_{xy} = \frac{V_2\ S_2}{I_1 t} + \frac{M_3}{\Omega t} + \frac{M_\omega S_\omega}{I_\omega\ t} \tag{27}$$

which is valid for closed sections and where t is the thickness of the considered concrete fibre inside cross section (in this case it is the web thickness); S_2 is the first moment (static moment) related to the concrete fibre and defined as per Jourawski theory; Ω the double of the area of internal box hollow (Bredt theory); S_ω the first moment (static moment) of sectorial areas with respect to shear centre C. For open sections the value of tangential stress due to Saint-Venant theory has to be substituted to that of Bredt theory.
Figure 4 shows the stress state due to torsional warping.

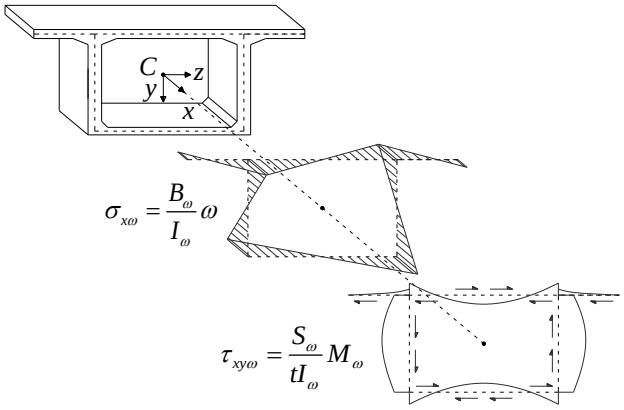

Figure 4. Typical stress state due to torsional warping

3 CASE-STUDY

The analysis of the launching stages of a bridge of four spans of equal length l_{JK} = 46 m is proposed. The bridge is horizontally curved with a constant radius R = 200m, total length of the deck L_{tot} = 184 m. Two different construction sequences are supposed. In the first case (*a*) it will be assumed that the bridge is pushed with its entire box section over the four spans ; consequently the nose length is fixed equal to l_n = 28 m (about 60% of the span length). In the second case (*b*) it will be assumed instead that the bridge is pushed with only the U-section of the lower body, without the upper slab, using four temporary piers placed in the middle of the spans, in order to lead to 8 spans , for a reduced length l_{JK} = 23 m and a nose length l_n = 14 m. This in order to compare and optimize the effects of the launch with the two different construction methods, evaluating the behavior of the closed and open sections and to compare the launch of the entire deck section (which assumes the use of very onerous work equipment) with that of reduced section, involving reduced weight and equipment.

All construction phases were analyzed using the methodology described above. The geometric properties of the bridge are shown in figure 5 and the numerical values are given in Table 1 for the two sections considered.

In both cases stiffeners occur with spacing of 6 m along the beam in order to reduce the effects of cross section distortion and to restrict the distortional axial stress under the 5% as indicated in some guidelines for curved bridges. In addition, rigid diaphragms that prevent torsional warping are placed in those sections that, in the final scheme, will be placed over the piers and abutments. In this analysis the effect of shear-lag has been neglected even if in the box or Π section it may increase the values of axial stresses in the areas of flanges close to webs.

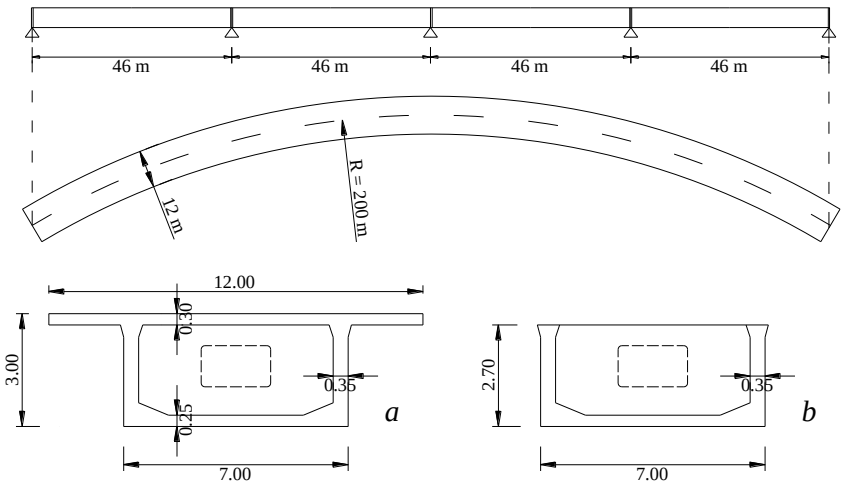

Figure 5. Geometric properties of the bridge [m]

In this study only the effect of non-uniform torsion will be taken into account, thus neglecting distortion (loss of shape) and shear-lag. Results are reported through envelope diagrams of internal forces and stresses. The values of shear force V_2 and total twisting moment M_3 (primary M_d and secondary M_ω) are useful for the evaluation of shear stresses, while bending moment M_1 and bimoment B_3 allow the evaluation of the maximum and minimum values of axial stresses. This is necessary to perform the safety checks of deck sections against cracking and to design the temporary prestressing of launching [1]. For the sake of brevity, diagrams of primary torsion M_d and secondary torsion M_ω are not reported, even though they can be derived from the analysis as well as the total moment M_3 and the bimoment B_3.

Table 1. Geometric properties of the cross sections considered

		Box section (case a)	U-shape section (case b)	Nose
E	[MPa]	36000.0	36000.0	210000
G	[MPa]	15000.0	15000.0	87500
p_2	[kN/m]	195	90	45
A	[m^2]	7.065	3.460	0.465
J_1	[m^4]	9.942	2.445	0.226
J	[m^4]	20.416	0.106	0.001
J_c	[m^4]	30.418	-	-
I_ω	[m^6]	11.985	18.706	2.068
κ		0.329	1	1
y_e	[m]	1.159	1.901	0.800
y_i	[m]	1.841	0.793	0.800
ω_e	[m^2]	2.018	3.262	3.900
ω_i	[m^2]	2.657	5.301	3.900

Figure 6 shows an example of the superposition of bending moment and twisting moment diagrams for several launching steps over a span of the bridge. The related envelope diagrams are obtained by repeating the bridge analysis for steps of launching increment of 1 m and shifting all diagrams obtained in the final configuration of the bridge, giving the maximum and minimum values of internal forces in every section for the entire launching sequence.

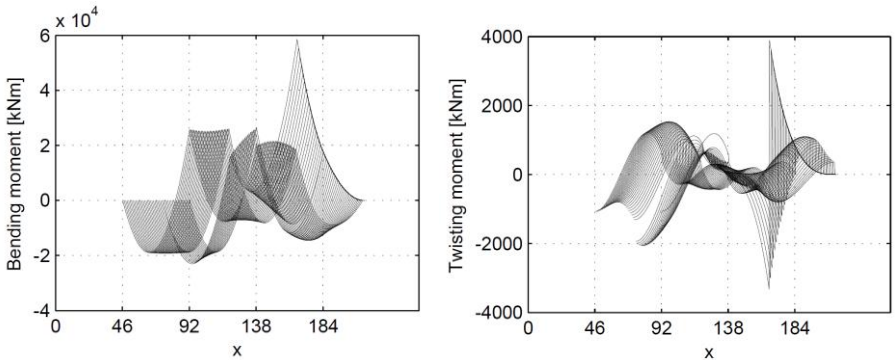

Figure 6. Example of superposition of internal force diagrams for several launching steps of a span and for the deck with steel I-girders

3.1 Whole prestressed box section

Figure 7 shows the envelope diagrams of shear force V_2, bending moment M_1, total twisting moment M_3 and bimoment B_3 in the case of the box concrete cross section. The envelope diagrams are obtained by repeating the analysis of the bridge for steps of advancement of 1 m and translating all the diagrams obtained in the final configuration, finding the maximum and minimum values of the stresses in each section for the entire launching sequence. The beam segment over the length of 184 m is the one related to the steel nose. It is worth noting that the maximum values of bending moment and twisting moment are placed in correspondence of the first segments launched, from 138 to 184 m. The values of bimoment are low along the entire deck, with maximum values in correspondence of the nose, because the closed section is generally less sensitive to non-uniform torsion than the open section (I-girders), used for the nose. Please note the peaks of bimoment over pier sections, which are also the sections in which the rigid diaphragms are placed during the advancement, with the highest value obtained in the joint section between the nose and the deck.

Figure 8 shows the diagrams of the axial stresses given by the sum of the effects of bending moment and bimoment, obtained by applying eq. (26) without prestressing. In Figure 8, the last segment related to the nose has been eliminated, thus showing only the stress diagram on the concrete deck, which is useful for the design of temporary prestressing in the early stages of construction. The maximum values of stress are placed in the most forwarded

part of the bridge (front zone), with high values of tensile stresses for the entire deck length and similar values at the intrados (*i*) and extrados (*e*) of cross section.

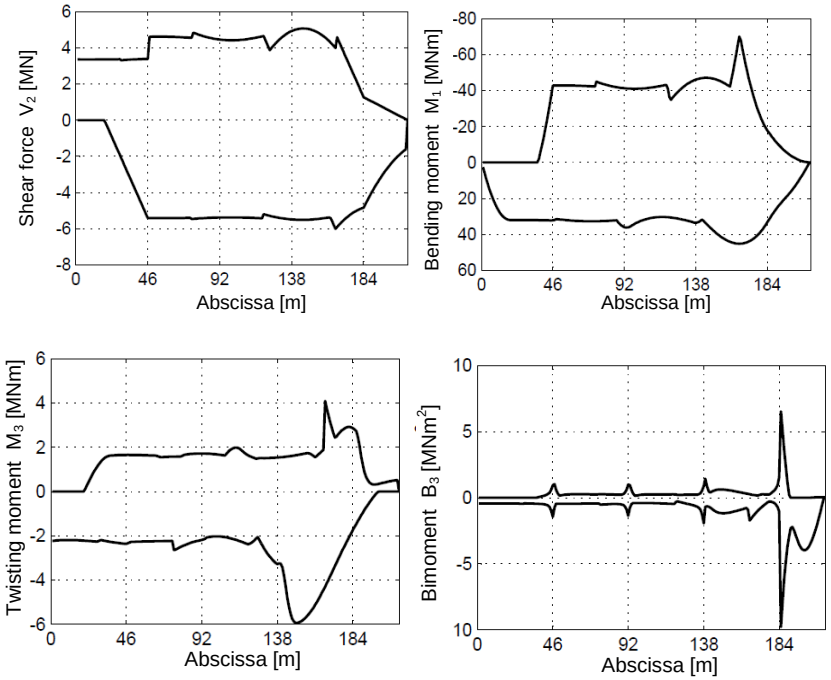

Figure 7. Envelope diagrams for box girder: shear force, bending moment, total twisting moment and bimoment

In curved bridges, the presence of internal prestressing tendons generates a distributed transverse force P/R, being P the value of the prestressing force [27,28]. When these transverse forces are eccentric with respect to the shear center, a significant value of twisting moment has to be added. Centered prestressing generates instead a limited value of torsion, attributable only to the eccentricity between the centroid of tendons and the shear center, which generally can be neglected. In addition, the transverse forces acting to the deck generate a beneficial "arch effect" in the horizontal plane (if the end restraints are able to prevent the transverse displacements), and this effect gives a limited value of the axial stress, which can be seen as a secondary effect of centered prestressing in curved bridges. Axial stresses due to bimoment contribute for about 5-8 % to the total value, confirming that in this case non- uniform torsion may be significant only in the areas close to diaphragms. Applying eq. (27) tangential stresses due to torsion can be obtained and combined with those due to shear, in order to verify if the transverse reinforcement designed for the

service loads are appropriate also in construction stages. Reinforcements for prestressed concrete box girders are evaluated in [29] taking into account the interaction between longitudinal shear, torsion and transverse bending.

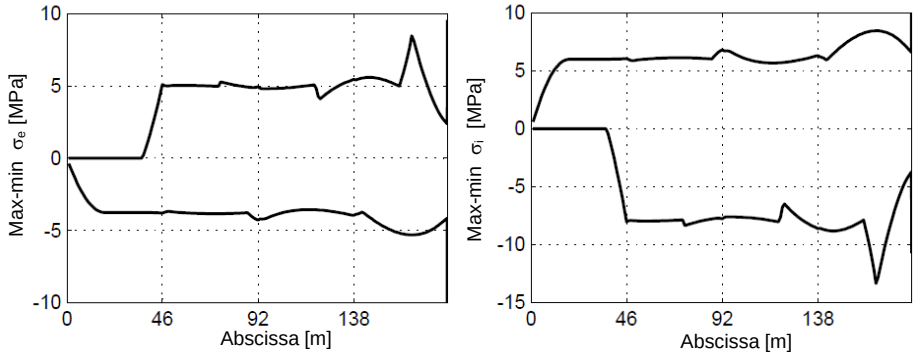

Figure 8. Envelope diagrams of axial stresses at the intrados and extrados of box girder

3.2 U-shape prestressed open section

For the case of the deck construction in two phases, with the advancement of the U-shaped section and the later cast of the upper slab, the launching steps are here analyzed for a comparison with the previous results, in which the whole box section is launched. In this second case, temporary piers reduce the span length to the half of the previous ones. Incrementally launched U-shaped girders are nowadays frequently built and they have been studied recently in [30].

Figure 9 shows the envelope diagrams of internal forces. The incidence of bimoment is evident here, the open section being much more sensitive to the effects of non-uniform torsion. The shape of the envelope diagrams of twisting moment and bimoment are very different from that of the corresponding situation depicted for the previous case in figure 7. This is due to the greater number of spans and to the U-shaped open section, more sensitive to non-uniform torsion. Although the total values are significantly diminished due to the reduction of weights and lengths of launch, the incidence of torsion and bimoment are very evident throughout the entire deck, for any launching stage. The negative peak of bending moment due to the cantilever phases is also very pronounced, in the sections between 161 m and 184 m.

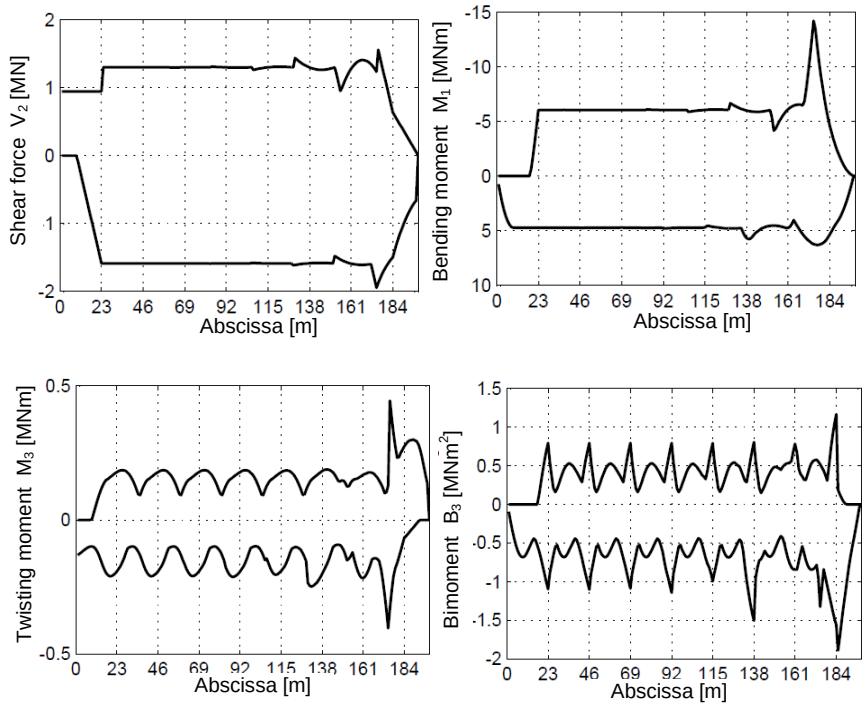

Figure 9. Envelope diagrams for U-shaped girder: shear force, bending moment, total twisting moment and bimoment

Figure 10 shows the envelope diagrams of the axial stresses. The high value of tensile stresses at the lower edge of the section indicates that prestressing reinforcement has to be lowered, giving more compression at the bottom fiber.

On the other hand in the case of the U-shaped section, the shear center lies below the bottom slab, indicating that temporary prestressing has to be lowered as much as possible, even though the total value of prestressing is expected lower than in the previous case. The contribution of non-uniform torsion is significant, with a percentage of axial stresses due to bimoment varying in the range 10-20 %.

The shape of the envelope diagram of fig. 10, which turns out to be much more rugged than the previous case of fig. 8, indicates that the contribution of the stresses due to bimoment in slabs, overlaps with that of the bending moment appreciably.

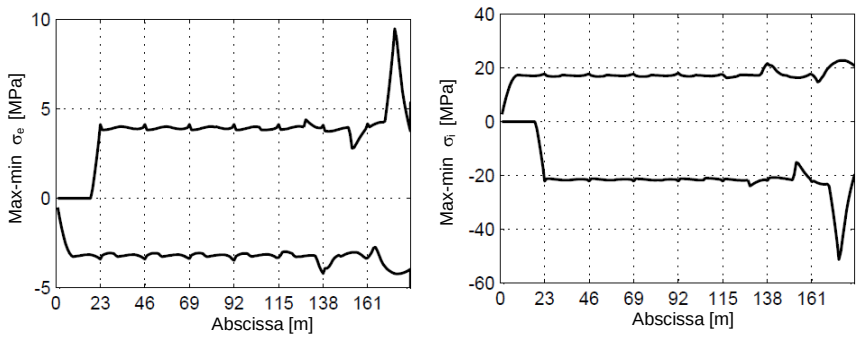

Figure 10. Envelope diagrams of axial stresses at the intrados and extrados of the U-shaped girder

From a comparison of provisional prestressing in the two cases examined, it is shown that the maximum tensile stress in the current zone is about 7.0 MPa for the box girder and 20.0 MPa for the U-shaped deck. In the first case a centered prestressing with a maximum of 20 tendons (made of 15 strands 0.6") has been considered, while in the second case a bottom prestressing (eccentrically applied) with a maximum of 15 tendons has been considered.

4 CONCLUSIONS

In this study the analysis of construction stages of concrete curved incrementally launched bridges was presented, with the aim of evaluating the effects of secondary torsion in two different methodologies of launching. In the first one the bridge deck is launched with its whole box section while in the second case, the deck is launched with a partial section, U-shaped, without the upper slab. The second hypothesis leads to the need of reducing the span lengths through the use of provisional piers. The purpose is to compare the two different procedures and the consequences on the design phase. In the case with the whole box section, the launching equipment is very onerous and provisional prestressing is highest. In the case of U-shaped section, the additional cost of temporary piers has to be considered but a reduction of launching equipment and temporary prestressing occurs.

The analysis was addressed by the Hamiltonian Structural Analysis method, providing a unified theory of the generalized beam for open and closed thin-walled sections. The proposed method is particularly effective in the case of incrementally launched bridges for the speed of analysis of a large number of static schemes that follow one another during the advancement, obtaining envelope diagrams of internal forces and stresses.

The influence of secondary torsion in the two cases was evaluated. Although in international codes the significance of torsional warping is generally restricted to open sections, Murìn et al. [17] and the authors [21] found that the

effects of secondary torsion can be important also in beams with closed sections. For the case-study analysed in the present paper, incrementally launched bridges with box sections show a percentage of axial stresses due to bimoment up to 5-8% in the areas close to the diaphragms. By contrast in U-shaped sections the contribution of bimoment to axial stresses rises to 10-20 %. The evaluation of axial and tangential stresses is of particular importance for establishing the temporary launching prestressing and the transverse reinforcements.

REFERENCES

[1] Rosignoli M. (2014) *Bridge Launching*, 2nd ed., ICE Publishing, Thomas Telford, London.
[2] Marchetti M.E. (1984) "Specific design problems related to bridges built by using the incremental launching method", *Engineering Structures*, **6**, 185-210
[3] Favre R., Badoux M., Burdet O., Laurencet P. (1999) "Design of a Curved Incrementally Launched Bridge", *Structural Engineering International IABSE*, **2**, 128-132.
[4] Vlasov V.Z. (1961) *Thin-walled Elastic Beams*, 2nd ed. (Israel Program for Scientific Translation).
[5] Dabrowski R. (1965) "Wölbkrafttorsion von gekrümmten Kastenträgern mit nichtverformbarem Profil.", *Der Stahlbau*, 34(5), 135-141 (in German).
[6] Bažant Z.P. (1965). "Non-uniform torsion in thin-walled bars of variable cross-section", *Publications International Association for Bridge and Structural Engineering IABSE*, **25**, 245-267, Zurich.
[7] Sedlacek G. (1969) "Zur Berechnung der Spannungsverteilung in dünnwandingen Stäben unter Berücksichtigung der Profilverformungen". (Analysis of stress distribution in thin-walled beams considering deformation of cross section). *Der Stahlbau*, 38(10), 314-320.
[8] Kollbrunner C.F., Basler K. (1969) *Torsion in structures*. Springer-Verlag, Berlin.
[9] Kollbrunner C.F., Hajdin N. (1975) *Dünnwandigen Stäbe*. Vol. 2, Springer-Verlag, 284 pp.
[10] Guo Zhong-heng (1981) "A unified theory of thin-walled elastic structures", *J. Struct. Mech*., **9**(2), 179-197
[11] Bažant Z.P., El-Nimeiri M. (1974). "Stiffness method for curved box girders at initial stress", *Journal of Structural Division ASCE*, **100**(10), 2071-2090.
[12] Razaqpur A.G.& and Li H.G. (1994), "Refined Analysis of Curved Thin-Walled Multicell Box Girders", *Computers and Structures*, **5**(1), 131-142
[13] Nakai H., Yoo H. (1988) *Analysis and design of curved steel bridges*. McGraw-Hill, N.Y.
[14] Maisel B.I. (1985) "Analysis of concrete box beams using small computer capacity", *Canadian Journal of Civil Engineering*, **12**(2), 265-278.
[15] Murín J., Kutis V. (2008) "An effective finite element for torsion of constant cross-sections including warping with secondary torsional moment deformation effect". *Engineering Structures*, 30, 2716–2723.
[16] Mokos V.G., Sapountzakis E.J. (2011) "Secondary torsional moment deformation effect by BEM", *International Journal of Mechanical Sciences*, **53**, 897-909
[17] Murín J., Aminbaghai M., Kutiš V., Královic V., Sedlár T., Goga V., Mang H. (2014) "A new 3D Timoshenko finite beam element including non-uniform torsion of open and closed cross sections", *Engineering Structures*, **59**, 153–160.
[18] Sapountzakis E.J., Tsiptsis I.N. (2015) "Generalized warping analysis of curved beams by BEM", *Engineering Structures*, **100**, 535–549
[19] Arici M., Granata M.F. (2016). "Unified theory for analysis of curved thin-walled girders with open and closed cross section through HSA method", *Engineering Structures*, 113, 299-314, ISSN: 0141-0296, doi: 10.1016/j.engstruct. 2016.01.051.

[20] Zhong Wan-Xie (2004) *Duality system in applied mechanics and optimal control*. Kluwer Academic Publishers. 456 pp.
[21] Arici M., Granata M.F., Oliva M. (2015) "Influence of secondary torsion on curved steel girder bridges with box and I-girder cross-sections", *KSCE Journal of Civil Engineering*, **19**(7), 2157-2171, doi: 10.1007/s12205-015-1373-1.
[22] Rosignoli M. (1997) "Solution of the continuous beam in launched bridges", *Proc. Instn. Civ. Engrs. Structs. & Bldgs*, **122**, 390-398.
[23] Sasmal S., Ramanjaneyulu K. (2006) "Transfer matrix method for construction phase analysis of incrementally launched prestressed concrete bridges", *Engineering Structures*, **28**, 1987-1910.
[24] Fontan A.N., Diaz J.M., Baldomir A., Hernandez S. (2011) "Improved optimization formulations for launching nose of incrementally launched prestressed concrete bridges", *Journal of Bridge Engineering ASCE*, **16**(3), 461-470.
[25] Granata M.F., Margiotta P., Arici M. (2013) "A parametric study of curved incrementally launched bridges", *Engineering Structures*, **49**, 373-384.
[26] Granata M.F. (2014). "Analysis of non-uniform torsion in curved incrementally launched bridges". *Engineering Structures*, **75**, 374-387, ISSN:0141-0296, doi: 10.1016/j.engstruct. 2014.05.047.
[27] Menn C. (1990) *Prestressed Concrete Bridges*, Springer-Verlag, Wien.
[28] Manterola Armisen J. (2006) *Puentes: apuntes para su diseño, cálculo y contrucción*, Esc. Tec. Sup. de Ingenieros de Caminos, Canales y Puertos. Madrid.
[29] Recupero A., Granata M.F., Culotta G., Arici M. (2016) "Interaction between longitudinal shear and transverse bending in prestressed concrete box girders", *Journal of Bridge Engineering ASCE*, in publication.
[30] Wang J.F., Lin J.P., Fan X.L. (2015) "Evaluation of Long Multi-Span Steel U-Shaped Girder During Incremental Launching Construction", *Journal of Testing and Evaluation ASTM*, 43(2), DOI: 10.1520/JTE20140123